PERGAMON

Energy Conversion and Management 43 (2002) 135–150

ENERGY CONVERSION & MANAGEMENT

www.elsevier.com/locate/enconman

Back absorbing parallel plate polymer absorbers in solar collector design

P.T. Tsilingiris

Department of Energy Engineering, Technological Educational Institution (TEI) of Athens, A. Spiridonos Street GR 122 10, Egaleo, Athens, Greece

Received 23 December 1999; received in revised form 26 September 2000; accepted 27 January 2001

Abstract

Serious efforts are currently devoted towards making solar water heating technology economically competitive. Among them, the development of large, all plastic, innovative design, low cost collector modules suitable for mass production is one of the most promising, which will eventually lead to a drastic reduction of the solar collector subsystem cost. Although appreciable development work was earlier devoted towards production of all plastic solar collectors, the polymer absorber still remains the most crucial part of the polymer collector design, since severe limitations are imposed by the low thermal conductivity of polymers. To overcome these restrictions, a suitable design should be implemented, allowing extended wetted surfaces of the absorbers, something which leads to the familiar extruded parallel polymer plate absorber design. Recent investigations have been directed toward definition of the limitations and development of design criteria for the top absorbing parallel polymer plate absorber. In the present work, a subsequent analysis is developed for evaluation of the back absorbing polymer plate design, which allows the absorption of radiation at the water stream and the back plate. The results of the current analysis, which are presented comparatively to those obtained for the top absorbing plate design, show a remarkable improvement of the collector efficiency factor and a corresponding reduction of the collector loss coefficient, something which leads to a significant improvement of the instantaneous heat collection efficiency of collectors using a back absorbing plate absorber design.

Keywords: Solar polymer absorber; Collector efficiency factor; Collector loss coefficient

1. Introduction

The economic viability of solar thermal conversion technology in the rapidly developing free energy market environment will be based on its competitiveness against conventional energy. The

0196-8904/02/$ - see front matter
PII: S0196-8904(01)00015-2

Nomenclature

A	area (m^2)
b	plate thickness (m)
d	plate spacing (m)
C	numerical constant
D	diameter (m)
F'	collector efficiency factor
h	convective heat transfer coefficient ($W\,m^{-2}\,K^{-1}$)
k	thermal conductivity ($W\,m^{-1}\,K^{-1}$)
l	thermal expansion coefficient (K^{-1})
L	length (m)
$\dot{m}$	unit area mass flow rate ($kg\,m^{-2}\,s^{-1}$)
m	numerical constant
$\dot{M}$	mass flow rate ($kg\,s^{-1}$)
n	numerical constant
P	perimeter (m)
q	unit area energy rate ($W\,m^{-2}$)
S	solar energy absorption ($W\,m^{-2}$)
T	temperature (°C or K)
U	loss coefficient ($W\,m^{-2}\,K^{-1}$)
V	flow velocity ($m\,s^{-1}$)
W	width (m)

Greeks

μ	viscosity ($kg\,m^{-1}\,s^{-1}$)
v	kinematic viscosity ($m^2\,s^{-1}$)
ρ	density ($kg\,m^{-3}$)

Subscripts

a	ambient
b	back, back plate
bf	back plate-fluid interface
c	collector
f	fluid
f1	top plate-fluid
f2	back plate-fluid
h	hydraulic
L	loss
p	top plate
pf	top plate-fluid interface
t	top
u	useful gain

relatively low cost of conventional energy during the last decade indicates that the role of developing simple, reliable and low cost systems, employing widely available recyclable materials, will be decisive for the future of this technology.

The cost reduction of solar heating plants should mainly be based on drastic cost reduction of the collector field subsystem. Towards this aim, the development of modular, innovative design, all polymer, low cost collectors will eventually allow easy and low cost construction of large collector fields with a significant material, labour and plumbing cost reduction. Innovative designs of all polymer collectors have been earlier and more recently proposed and demonstrated [1–4].

According to the theory [5], the useful heat gain of a solar collector can simply be expressed as a function of the mean absorber plate temperature. To allow reference to a localized fluid temperature, the collector efficiency factor F' is defined in the familiar Hottel–Willier–Bliss model. Derivation of this factor, which may remarkably affect the collector performance parameters, is based on the assumption of a negligible thermal resistance between the absorber plate and the heat removing fluid. Although this assumption is adequately satisfied for collectors with metal absorbers, it is not always valid for collectors with polymer absorbers with a considerably lower thermal conductivity. Although the use of polymer materials is currently considered very promising for development of large, all plastic solar collector arrays at a remarkably lower cost using mass production processes, their low thermal conductivity may strongly affect the solar absorber efficiency and deteriorate the collector performance, unless a special absorber design is implemented.

Among them, the most promising is the extruded parallel polymer plate absorber design, which is basically composed of a pair of parallel plates at the top surface of which the incident solar radiation is absorbed. The dissipated heat is transferred through the top polymer plate via conduction into a water stream flowing between the plates. The spacing between the plates can, typically, vary from a few millimeters to a few centimeters, depending on the particular collector design. In a recent investigation [6], a heat transfer analysis was performed, which allowed the development of specific design criteria and evaluation of the collector performance parameters for this particular absorber design. However, since the top plate conductance is proportional to the thermal conductivity of the polymer material and inversely proportional to the plate thickness, a performance improvement would be expected by a significant reduction of the top absorbing plate thickness, something which is usually impossible, owing to mechanical reasons.

However, it would be possible to avoid the undesirable effects of the poor thermal conductance of the top absorbing plate, alternatively by replacing the top dark absorbing plate by a transparent plate. This absorber design allows partial absorption of the incident solar radiation directly by the flowing water stream and by the dark surface of the back polymer plate.

The purpose of this work is to present an analysis for evaluation of the collector performance parameters for back absorbing polymer absorbers. The collector performance parameters, in particular the collector efficiency factor and the modified collector loss coefficient in the familiar Hottel–Willier–Bliss model, strongly determines the instantaneous heat collection efficiency of solar collectors. The paper also aims to compare both polymer absorber designs through the presentation of comparative performance parameters and collector efficiencies of typical solar collectors with back and top absorbing plate absorbers.

2. Material considerations on absorber design

Polymers are widely available, low cost materials, which lend themselves to volume production of lightweight, low cost collectors, tolerant to corrosion and freezing temperatures. Many surveys and reports have been focussed on polymers as solar collector materials [7,8]. However, their reliability, durability and long term performance have not generally been fully demonstrated yet for solar heating plants. Since polymer glazings are subject to degradation under the exposure to UV radiation, glass panes were alternatively proposed. Glass not only eliminates the possibility of rapid degradation of the polymer glazing system under environmental exposure but also offers additional UV protection for the collector absorber.

A brief review of the thermophysical properties of widely available candidate polymer materials, as derived from various sources [9–11], is presented in Table 1. It is clear that the service temperature determines the application range of the polymer collectors, which can undoubtedly be employed, not only for low and medium service temperatures, up to 50°C, and between 50°C and 80°C, respectively, but also marginally for high (above 80°C) temperatures. The most suitable polymer materials for absorber design have been proved to be those of the polyolefin group, like polyethylene and polypropylene, and of the ethylene–propylene–diene–monomer (EPDM) group, known as synthetic rubbers. The polyolefins are mainly suitable for manufacturing thermally extruded flat rigid absorbers. Flexible tubes or tube strips interconnected by flexible webs, suitable for low temperature unglazed pool heaters, have been tested and are being manufactured of EPDM.

It is important that the high expansion coefficient of polymers should be taken into consideration in the absorber and solar collector design. There is also a relatively significant variation of thermal conductivity between the various polymer materials. For example, the thermal conductivity of high density polyethylene is almost three times as high as that of EPDM. However, it

Table 1
Thermophysical properties of various polymer materials (adapted from Refs. [9–11])

Material group	Thermo-physical property	Material designation			
		Low density	Medium density	High density	Ultra high density
Polyolefins	k_p ($W\,m^{-1}\,K^{-1}$) (ASTM C177)	0.33	0.33–0.419	0.46–0.52	0.46
	l (K^{-1}) coefficient of thermal expansion (ASTM D696)	$10–22 \times 10^{-5}$	$14–16 \times 10^{-5}$	$11–13 \times 10^{-5}$	14×10^{-5}
	T_{max} (°C) Recommended maximum temperature	82–100	104–121	121	–
EPDM	k_p ($W\,m^{-1}\,K^{-1}$)	0.138–0.159			
	1 (K^{-1})	12×10^{-5}			
	T_{max} (°C) Recommended maximum temperature	125			

should also be noted that the thermal conductivity of most widely available polymers is, on average, almost three orders of magnitude lower than that of metallic absorber materials, something which makes the complete redesign of the conventional metal absorber absolutely necessary.

In recent absorber designs, in order to overcome the poor thermal conductivity of polymer materials, special attention is concentrated towards increasing the absorber surface in direct contact with the heat transfer fluid. This is known as the fully wetted absorber design. A good report on the design of polymer absorbers was provided by Madsen and Goss [12]. Among the proposed polymer absorber designs are the EPDM parallel tube design, which was extensively employed as low temperature swimming pool heating collectors, the polymer film water bag absorber in glazed or unglazed collectors and the extruded polymer absorbers offering both good mechanical rigidity as well as extended wetted surfaces for optimal heat transfer.

Several design alterations and improvements have been proposed for improved mechanical rigidity of extruded polymer plate absorbers, like the rib connection of plates to withstand hydrostatic forces.

3. Theoretical model and analysis

The model of an ordinary flat plate collector with an extruded back absorbing plate polymer absorber is shown in Fig. 1, along with the location of the nodes in the corresponding thermal network. The parallel plates of thickness b are located at a distance d apart, and the single glass pane glazing, as well as the collector back insulation, are also shown in this figure. The transparent top polymer plate allows transmission of the incident solar radiation and absorption in both the back absorbing plate and in the water flowing stream. The dissipated solar heat at the

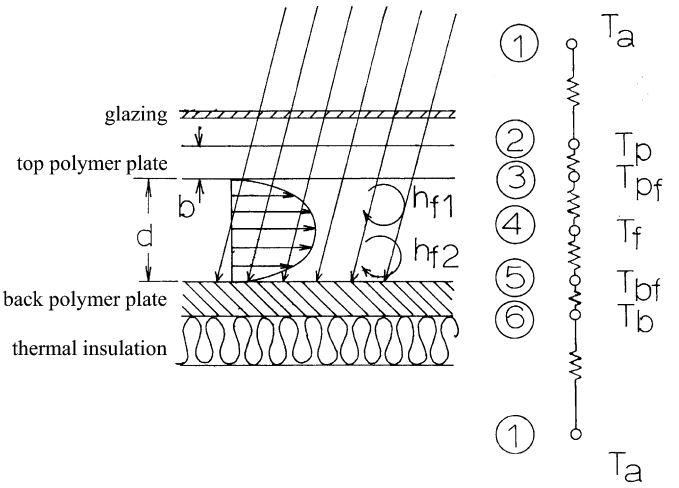

Fig. 1. The model of a single glazed solar collector with a back absorbing parallel plate polymer absorber. In the same plot, the location of nodes of the associated thermal network is shown. Both absorber plates are of thickness b, and they are located at distance d apart (thicknesses not to scale).

back polymer plate is transferred by convection to the fluid stream and by combined convection conduction and radiation to the ambient air through the top polymer plate and glazing system. Additional heat losses also occur via conduction and convection radiation through the back polymer plate and thermal insulation to the environment. The heat flow through the polymer plates is assumed to be one dimensional, owing to the large lateral dimensions of the collector module and to the adequate thermal insulation at the collector periphery.

The spectral extinction coefficient of glass, especially of low iron content quality, is almost uniform at the visible and near Infrared (IR) band of the solar spectrum [13]. According to the existing literature [14,15], although the spectral extinction coefficient of most commercially available transparent polymer films and plates varies considerably, depending on their particular type and chemical composition, in the far IR spectrum, it can be taken as uniform in the visible and near IR without significant loss of accuracy. The incident solar radiation undergoes a slight, almost spectrally uniform extinction at the top glass and polymer plates before entering the water flow passage. This amount of energy absorption will be completely ignored in the present analysis, because of either the low extinction coefficient or the small thickness of the parallel transparent regions, as is usually assumed in solar collector theory.

The water, however, is a strongly selective absorber with very high extinction coefficients around a high transmittance window near 0.5 μm. This leads to a substantial selective absorption at the near and far IR part of the solar spectrum, which should be considered explicitly in the calculations.

The convective heat transfer coefficient between the top or bottom polymer plates and the heat transfer fluid may vary considerably, depending on the particular absorber design or operating conditions and mass flow rates. This is due to the fact that for a particular hydraulic diameter of flow passage, defined as $D = 4A/P$ where A and P are the cross-section area and the wetted perimeter, respectively, and the particular mass flow rate, the Reynolds number may vary considerably. For the extended lateral dimensions of the absorber plate, as happens in the ordinary flat plate collectors, the rib connection of the polymer plates is proved to be absolutely necessary to withstand the mechanical loads of hydrostatic origin. However, the presence of ribbing between the plates, which splits the heat transfer fluid flow into a number of parallel streams, is not expected to present any significant flow or thermal effects, owing to their small ribbing conductance. Therefore, the effect of the usual rib connections at a fairly long distance apart will be completely ignored in the subsequent analysis without any significant loss of accuracy.

The hydraulic diameter of a rectangular flow passage of width W is calculated as

$$D = 2d/(1 + d/W) \tag{1}$$

where d the absorber polymer plate spacing. When $(d/W) \to 0$, as usually happens in practice, the hydraulic diameter becomes $2d$. Assuming that the mass flow rate through the whole absorber area is $\dot{M}$ and the absorber cross-sectional area is $A = dW$, where W is the width of absorber, the average fluid velocity will be calculated as,

$$\bar{V} = \dot{M}/(\rho A) \tag{2}$$

The corresponding Reynolds number will be estimated as

$$\mathrm{Re} = \bar{V}2d/v = 2\dot{M}/(\mu W) \tag{3}$$

However, instead of the mass flow rate, the per unit collector area mass flow rate is usually employed in solar collector theory, defined as

$$\dot{m} = \dot{M}/A_c \tag{4}$$

Assuming that the collector absorber area is $A_c = WL$, the Reynolds number for the flow of the heat transfer fluid in the absorber becomes,

$$\mathrm{Re} = (2L/\mu)\dot{m} \tag{5}$$

Assuming the usual collector mass flow per unit area rates to range between 0.01 and 0.02 $\mathrm{kg\,m^{-2}\,s^{-1}}$, for large area polymer collector modules with a spacing between plates of about 0.01 m and width to length proportions in the order of 3×3 $\mathrm{m^2}$, the flow is expected to be laminar, and the entry flow length, being between 0.2 and 0.3 m, is expected to be a very small fraction of the collector length. For the laminar flow regime, the theory [16] predicts that the Nusselt number is independent of the fluid velocity and Reynolds number. Therefore, for a characteristic length equivalent to the typical plate spacing and for the thermophysical properties of water at typical operating temperatures, the heat transfer coefficient corresponding to a circular cross-section is estimated to be around 150 $\mathrm{W\,m^{-2}\,K^{-1}}$.

For lower mass flow rates, at the range between 0.001 and 0.005 $\mathrm{kg\,m^{-2}\,s^{-1}}$ corresponding to low flow collectors, no significant change of the estimated heat transfer coefficient is expected, while the entry length is expected to be an order of magnitude shorter.

For higher mass flow rates, which are, except for unusual absorber designs, rather unusual in practice, the Reynolds number for flow transition ($\mathrm{Re} = 2300$) may possibly be exceeded. In this case, the Nusselt number predicted by the theory, which for turbulent flow in circular cross-sections is given by the following familiar dimensionless correlation,

$$\mathrm{Nu} = C\,\mathrm{Re}^m Pr^n \tag{6}$$

with $C = 0.023$, $m = 4/5$ and $n = 1/3$, will be expected to be appreciably higher, corresponding to proportionally higher convective heat transfer coefficients.

However, for non-circular cross-sections with sharp corners and large aspect ratios, the fluid velocity and the corresponding local heat transfer coefficient may both vary appreciably around the periphery, approaching their minimum values at the corners. For these conditions, the Nusselt number for the fully developed flow should appropriately be corrected to account for the flow in rectangular cross-sections. The correction factors, proposed by the theory for a circular cross-section, to the Nusselt number are proportional to the aspect ratio of the cross-section [17], so the corrected Nusselt number and the corresponding convective heat transfer coefficient becomes, for a rectangular cross-section with $(d/W) \to 0$, about twice that expected for a circular cross-section.

Therefore, the subsequent analysis was performed for typical convective heat transfer coefficients of 75, 150 and 300 $\mathrm{W\,m^{-2}\,K^{-1}}$, which are expected to cover the whole typical parameter range for practical applications. The heat transfer fluid is assumed to be completely opaque to IR radiation, so the heat exchange between the top and back absorber plates can be completely ignored.

Referring to Fig. 1, in which the collector model and the thermal network are shown, the steady state heat balance equations for nodes 2–6 are,

$$U_t(T_p - T_a) - (k_p/b)(T_{pf} - T_p) = 0 \tag{7}$$

$$h_{f1}(T_f - T_{pf}) - (k_p/b)(T_{pf} - T_p) = 0 \tag{8}$$

$$h_{f2}(T_{bf} - T_f) + S_f - h_{f1}(T_f - T_{pf}) - q_0 = 0 \tag{9}$$

$$S_b - h_{f2}(T_{bf} - T_f) - (k_p/b)(T_{bf} - T_b) = 0 \tag{10}$$

$$(k_p/b)(T_{bf} - T_b) - U_b(T_b - T_a) = 0 \tag{11}$$

where S_f is the absorbed energy within the thin water layer, which is directly removed by the heat transfer fluid, and S_b is the energy absorption at the dark back polymer plate, which can be calculated by using ordinary ray tracing techniques. The spectral composition of diffuse radiation, which is usually shifted towards shorter wavelengths, is not generally similar to the direct radiation spectrum. For a first order approach, it would be adequate to assume a uniform spectral composition of both solar radiation components and to treat incident solar radiation as a beam without significant sacrifice of accuracy. The calculation of S_f and S_b is based on the nature of the optical processes in the solid semi-transparent, uniformly absorbing region and in the liquid strongly selective, absorbing parallel region. Radiation extinction phenomena in the selectively absorbing fluid layer depends strongly on its spectral extinction characteristics, as well as on the spectral composition of the incident energy. Although, in general, accurate transmission conditions are difficult to predict, several typical simple theoretical or experimental radiation transmission models have been proposed, which are bound by a theoretically calculated upper transmission model [18]. Although ray tracing techniques are suitable for application in relatively simple systems, they become extremely difficult to apply in more complex optical configurations with multiple parallel regions of materials with different optical characteristics in contact. In these cases and especially when absorption in parallel regions has to be taken into account explicitly, the effectiveness of the method becomes questionable, owing to the increased number of reflection and refraction paths. To overcome this problem, the net radiation method has been developed earlier and recently employed [19] to investigate the radiation absorption in an identical optical system with multiple parallel regions. The analysis is based on calculation of the incoming and outgoing energies at all optical interfaces, which can be directly employed for the calculation of S_f and S_b.

Elimination of the variables T_b, T_{bf}, T_{pf} and T_p from Eqs. (7)–(11) is possible, first by the elimination of T_p from Eqs. (7) and (8) to get

$$T_{pf} = \frac{(k_p/b)U_t T_a + h_{f1}(U_t + k_p/b)T_f}{(k_p/b)U_t + h_{f1}U_t + h_{f1}(k_p/b)} \tag{12}$$

In a similar way, eliminating the variable T_p from Eqs. (10) and (11) yields,

$$T_{bf} = \frac{S_b(U_b + k_p/b) + h_{f2}(U_b + k_p/b)T_f + (k_p/b)U_b T_a}{h_{f2}U_b + h_{f2}(k_p/b) + (k_p/b)U_b} \tag{13}$$

Solving Eq. (9) for $q_0 - S_f$ yields,

$$q_0 - S_f = T_{bf}h_{f2} + T_{pf}h_{f1} - T_f(h_{f1} + h_{f2}) \tag{14}$$

Substitution of T_{pf} and T_{bf} from Eqs. (12) and (13), respectively, in Eq. (14) and after rearrangements and algebraic manipulations yields,

$$q_0 - S_f = \frac{h_{f2}(U_b + k_p/b)S_b}{h_{f2}U_b + h_{f2}(k_p/b) + U_b(k_p/b)} - (k_p/b)\left(\frac{h_{f1}U_t}{h_{f1}U_t + h_{f1}(k_p/b) + U_t(k_p/b)} + \frac{h_{f2}U_b}{(k_p/b)U_b + h_{f2}U_b + h_{f2}(k_p/b)} \right)(T_f - T_a) \tag{15}$$

Modifying further Eq. (15) in a more convenient form finally yields,

$$q_0 - S_f = \frac{h_{f2}(U_b + k_p/b)}{h_{f2}(U_b + k_p/b) + U_b(k_p/b)} \left[S_b - \frac{k_p/b}{U_b + k_p/b} \times \left(U_b + U_t \frac{h_{f1}h_{f2}U_b + h_{f1}h_{f2}(k_p/b) + h_{f1}U_b(k_p/b)}{h_{f1}h_{f2}U_t + h_{f1}h_{f2}(k_p/b) + h_{f2}U_t(k_p/b)} \right)(T_f - T_a) \right] \tag{16}$$

The derived Eq. (16) is the familiar HWB equation which offers the useful heat gain of the collector,

$$q_0 - S_f = F'[S_b - U_L(T_f - T_a)] \tag{17}$$

where

$$F' = \frac{h_{f2}(U_b + k_p/b)}{h_{f2}(U_b + k_p/b) + U_b(k_p/b)} = \frac{1}{1 + \dfrac{U_b}{h_{f2}[U_b/(k_p/b) + 1]}} \tag{18}$$

and

$$U_L = \frac{(k_p/b)}{U_b + (k_p/b)} \left(U_b + U_t \frac{h_{f1}h_{f2}U_b + h_{f1}h_{f2}(k_p/b) + h_{f1}U_b(k_p/b)}{h_{f1}h_{f2}U_t + h_{f1}h_{f2}(k_p/b) + h_{f2}U_t(k_p/b)} \right) \tag{19}$$

Note that the collector efficiency factor F' in Eq. (18) depends solely on the back loss and convective heat transfer coefficients. For appreciably high values of (k_p/b), Eq. (18) simplifies to,

$$F' = \frac{1}{1 + U_b/h_{f2}} \tag{20}$$

which becomes close to unity when $h_{f2} \gg U_b$, as usually happens for a liquid heat transfer medium. For large enough values of the ratio (k_p/b) and $h_{f1} = h_{f2} = h_f$, Eq. (19) becomes

$$U_L = \frac{U_b + h_f}{U_t + h_f} U_t + U_b \tag{21}$$

in which, for $h_f \gg U_t$ and $h_f \gg U_b$, the ratio $(U_b + h_f)/(U_t + h_f)$ becomes close to unity and the collector loss coefficient becomes equal to the sum of the top and back loss collector coefficients, $U_t + U_b$.

4. Results and discussion

The collector efficiency factor, as determined from Eq. (18), is plotted in Fig. 2 against the parameter k_p/b for fixed heat transfer coefficients of $h_f = h_{f2} = 75$ (the pair of solid lines), 150 (the

pair of broken lines), 300 $\mathrm{W\,m^{-2}\,K^{-1}}$ (the pair of dotted lines) and $U_b = 2\ \mathrm{W\,m^{-2}\,K^{-1}}$ (top line) and $U_b = 4\ \mathrm{W\,m^{-2}\,K^{-1}}$ (lower line).

For each pair of fixed h_f lines, the curves of the lower U_b correspond to higher values of the collector efficiency factor F'.

By partial differentiation of Eq. (18) in terms of the independent variables U_b and h_{f2}, it is derived that,

$$(\partial F'/\partial U_b) = -h_{f2}(k_p/b)/[h_{f2}(U_b + k_p/b) + U_b(k_p/b)]^2 < 0 \tag{22}$$

and

$$(\partial F'/\partial h_{f2}) = U_b(k_p/b)(U_b + k_p/b)/[h_{f2}(U_b + k_p/b) + U_b(k_p/b)]^2 > 0 \tag{23}$$

which confirms the distribution of the curves in Fig. 2, showing that the collector efficiency factor, decreases as the back loss coefficient increases. It also confirms that it increases with a corresponding increase of the convective heat transfer coefficient.

It can also be seen that the collector efficiency factor is almost independent of the k_p/b ratio for the range of $200 < k_p/b < 1000$, irrespective of the parameter values of U_b and h_{f2}. However, an increase of plate thickness or decrease of plate thermal conductivity leads to a decrease of the plate conductance k_p/b. For lower values of the k_p/b ratio in the range of $0 < k_p/b < 200$, the collector efficiency factor increases, leading to higher useful collector heat gain. This is due to the additional thermal insulation of the low thermal conductance polymer plate, which contributes to reduction of the back collector insulation losses. It is also important to note, from the same figure and for $k_p/b < 200$, that this increase is stronger for higher values of U_b, irrespective of the parameter value of h_{f2}.

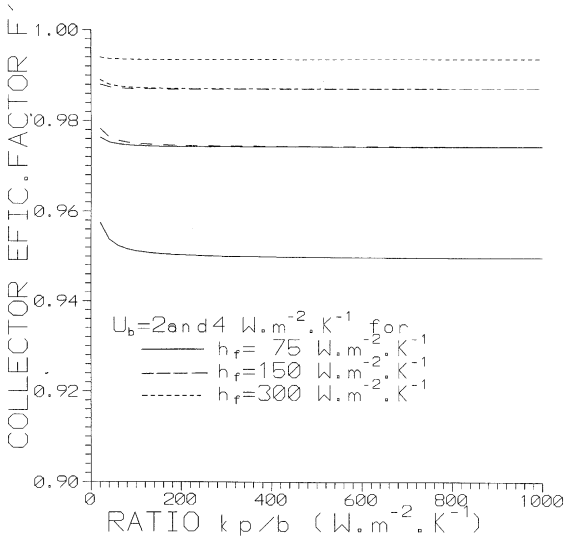

Fig. 2. The collector efficiency factor plotted against k_p/b for a back plate absorber design and convective heat transfer coefficients of $h_{f2} = 75$, 150 and 300 $\mathrm{W\,m^{-2}\,K^{-1}}$ corresponding to the solid, broken and dotted lines, respectively. The topmost of each of the pair of uniform h_f curves correspond to $U_b = 2$ while the second lower to $U_b = 4\ \mathrm{W\,m^{-2}\,K^{-1}}$.

In Figs. 3 and 4, the calculated collector loss coefficient given by Eq. (19) was plotted against the k_p/b ratio for top loss coefficients of $U_t = 3$, 5 and 7 $W m^{-2} K^{-1}$ and for fixed back loss coefficients of $U_b = 2$ (Fig. 3) and 4 $W m^{-2} K^{-1}$ (Fig. 4), respectively. The three solid, broken and dotted lines of each group of fixed top and back loss coefficients correspond to a convective heat transfer coefficient between the top or back plate and the heat transfer fluid of $h_{f1} = h_{f2} = h_f = 75$, 150 and 300 $W m^{-2} K^{-1}$, respectively. As the scales in both plots are the same, it can be seen clearly that the collector loss coefficient is more sensitive to the convective heat transfer coefficient

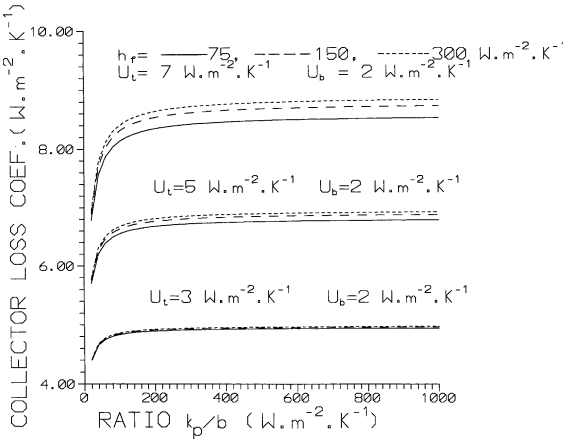

Fig. 3. The collector loss coefficient plotted as a function of k_p/b for convective heat transfer coefficients, as a parameter, of $h_{f1} = h_{f2} = h_f = 75$, 150 and 300 $W m^{-2} K^{-1}$ corresponding to solid, broken and dotted lines, respectively, as well as for top loss coefficients of $U_t = 3$, 5 and 7 $W m^{-2} K^{-1}$ and a fixed back loss coefficient of $U_b = 2$ $W m^{-2} K^{-1}$.

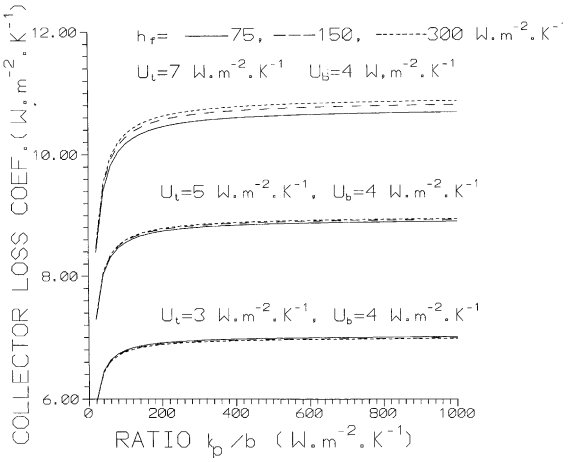

Fig. 4. The collector loss coefficient plotted as a function of k_p/b for a convective heat transfer coefficients, as a parameter, of $h_{f1} = h_{f2} = h_f = 75$, 150 and 300 $W m^{-2} K^{-1}$ corresponding to solid, broken and dotted lines, respectively, as well as for top loss coefficients of $U_t = 3$, 5 and 7 $W m^{-2} K^{-1}$ and a fixed back loss coefficient of $U_b = 4$ $W m^{-2} K^{-1}$.

for the lower figure of the back loss coefficient of 2 $W m^{-2} K^{-1}$, as it may comparatively be seen by the spacing between the fixed top loss coefficient lines of each group.

It can also be seen that although, for the region of $200 < k_p/b < 1000$, the collector loss coefficient is only slightly dependent on k_p/b, it sharply decreases for k_p/b much lower than 200. This is attributed to the initial assumption of negligible radiation absorption at the top transparent polymer region, owing either to a low extinction coefficient or a relatively small plate thickness. However, for very thick top polymer plates, the extinction, practically, cannot be assumed to be negligible. This may lead to significant absorption losses at the top transparent plate and reduction of the energy absorption at the back polymer plate, something which is expected to reduce the sharp decrease of the collector loss coefficient for $k_p/b < 200$ and will possibly tend to eliminate the performance improvement, owing to reduction of the absorber plate conductance.

To relax the assumptions of equal convective heat transfer coefficients between the top and back absorber plates and the heat transfer fluid, the calculations were repeated for the ratios $h_{f2}/h_{f1} = 0.5$ and $h_{f2}/h_{f1} = 2$ for a back convective heat transfer coefficient of $h_{f2} = 150$ $W m^{-2} K^{-1}$, and the results were plotted in Fig. 5. In this plot, the collector heat loss coefficient is shown as a function of the k_p/b ratio for a fixed back loss coefficient of $U_b = 2 W m^{-2} K^{-1}$ and top loss coefficients of $U_t = 3$, 5 and 7 $W m^{-2} K^{-1}$ as a parameter. In each group of lines, corresponding to $h_{f2}/h_{f1} = 0.5$ (broken lines) and $h_{f2}/h_{f1} = 2$ (dotted lines), additional results corresponding to $h_{f2}/h_{f1} = 1$ (solid lines) are also shown for comparison.

An inspection of Fig. 5 shows again the familiar behaviour of a sharp decrease of the collector loss coefficient in the region of $0 < k_p/b < 200$, as well as the effect of the parameters U_t and U_b on the collector loss coefficient. It can be seen clearly that the solid lines $h_{f1} = h_{f2} = 150$ $W m^{-2} K^{-1}$ are located, as expected, between the broken $h_{f1} = 300$ and dotted $h_{f1} = 75$ $W m^{-2} K^{-1}$ lines, re-

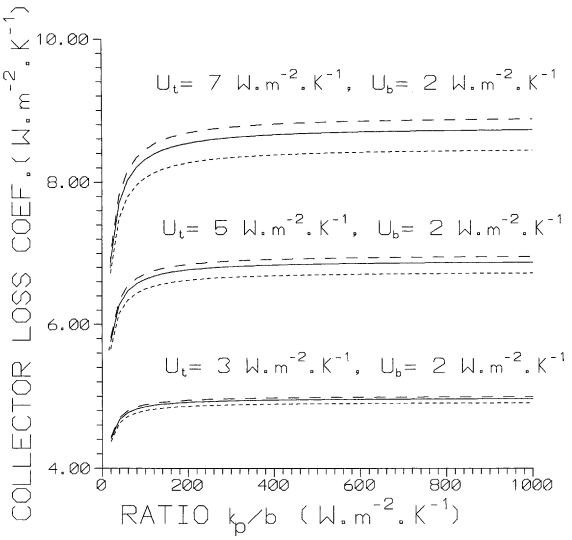

Fig. 5. The effect of convective heat transfer coefficient imbalance on collector loss coefficient plotted against k_p/b for $U_t = 3$, 5 and 7 $W m^{-2} K^{-1}$ and fixed $U_b = 2 W m^{-2} K^{-1}$ and $h_{f2} = 150$ $W m^{-2} K^{-1}$. Solid lines correspond to $h_{f2} = 150$ $W m^{-2} K^{-1}$ while broken and dotted lines correspond to $h_{f2} = 300$ and 75 $W m^{-2} K^{-1}$, respectively.

spectively, since higher or lower convective heat transfer coefficients between the top transparent plate and the fluid stream leads to higher or lower, respectively, top plate temperatures. The effect of the convective heat transfer coefficient from the top absorbing plate is stronger for the higher top loss coefficients, as seen by the spacing between the broken and dotted lines, owing to the proportionally higher top heat losses.

In Figs. 6 and 7, comparative results are presented for the collector efficiency factor F' and collector loss coefficient U_L, respectively, for the top and back absorbing plate polymer absorber design. The results of the current analysis are presented in both plots by solid lines compared with those of a recent investigation [6], corresponding to the alternative top absorbing plate design plotted by broken lines.

In Fig. 6, the collector efficiency factor is plotted as a function of k_p/b for a collector with $U_b = 4\ \mathrm{W\,m^{-2}\,K^{-1}}$ and $h_f = 150$ (top solid line) or 75 $\mathrm{W\,m^{-2}\,K^{-1}}$ (lower solid line). In the same plot, the corresponding values of the same parameter for the top absorbing plate design with $U_t = 7\ \mathrm{W\,m^{-2}\,K^{-1}}$ and $h_f = 150$ (top broken line) or 75 $\mathrm{W\,m^{-2}\,K^{-1}}$ (lower broken line) are comparatively shown. It is clear that not only the back absorbing plate absorber design leads to almost 20% higher F' values for the whole range between $200 < k_p/b < 1000$ but also leads to an opposite effect and far higher values of the same parameter in the range of $0 < k_p/b < 200$.

In Fig. 7, the collector loss coefficient U_L is plotted as a function of k_p/b for a collector with $U_t = 7$, $U_b = 4\ \mathrm{W\,m^{-2}\,K^{-1}}$ and $h_f = 150$ (top solid line) or 75 $\mathrm{W\,m^{-2}\,K^{-1}}$ (lower solid line). In the same plot, corresponding values of the same parameter U_L for the top absorbing plate absorber design are also comparatively shown for $h_f = 75$ (top broken line) or 150 $\mathrm{W\,m^{-2}\,K^{-1}}$ (lower broken line). It is clear that not only the collector loss coefficient for the back absorbing plate absorber design is, on average, 15% lower than the corresponding value for the top absorber plate

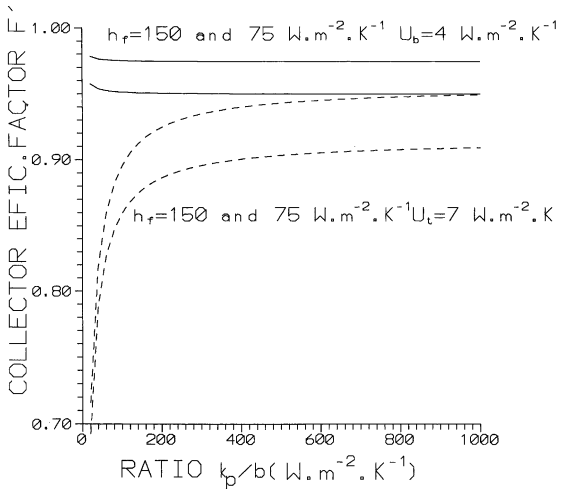

Fig. 6. Comparative presentation of the collector efficiency factor as a function of the ratio k_p/b for the back absorbing (solid lines) and top absorbing (broken lines) parallel plate polymer absorber designs for U_t and U_b fixed at 7 and 4 $\mathrm{W\,m^{-2}\,K^{-1}}$, respectively. The top line of each group corresponds to $h_f = 150\ \mathrm{W\,m^{-2}\,K^{-1}}$ while the lower line corresponds to $h_f = 75\ \mathrm{W\,m^{-2}\,K^{-1}}$.

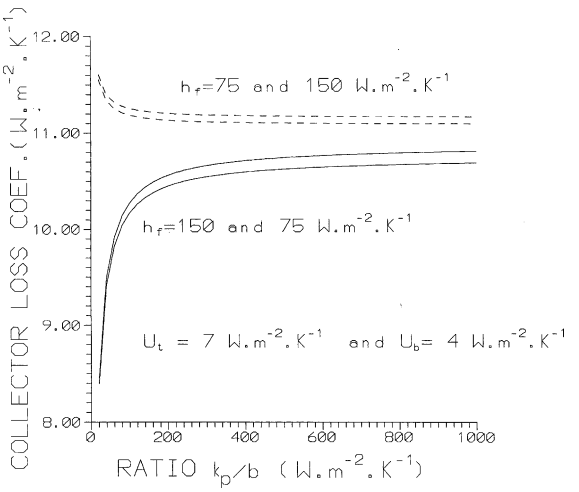

Fig. 7. Comparative presentation of the collector loss coefficient as a function of the ratio k_p/b for the back absorbing (solid lines) and top absorbing (broken lines) parallel plate polymer absorber designs for $U_t = 7\ \mathrm{W\,m^{-2}\,K^{-1}}$ and $U_b = 4\ \mathrm{W\,m^{-2}\,K^{-1}}$. The top and lower solid lines correspond to 150 and 75 while the top and lower broken lines correspond to 75 and 150 $\mathrm{W\,m^{-2}\,K^{-1}}$, respectively.

design in the range of $200 < k_p/b < 1000$ but also exhibits the same opposite effect and leads to far lower values of U_L for the very low values of k_p/b ranging between $0 < k_p/b < 200$.

Since the instantaneous heat collection efficiency of a solar collector is strongly determined by the performance parameters, through the linear Hottel–Willier–Bliss model, it would be important to quantify the collector performance improvement owing to the calculated higher values of U_L and F' for the back absorbing plate absorber design. For this reason, the efficiency lines corresponding to a collector with a back (solid line) and a top (broken line) absorbing plate absorber were plotted in Fig. 8 as a function of the ratio $(T_f - T_a)/G$ for fixed values of the collector performance parameters $(\tau\alpha)_n$ and U_L and for $k_p = 0.3\ \mathrm{W\,m^{-1}\,K^{-1}}$, $h_f = 100\ \mathrm{W\,m^{-2}\,K^{-1}}$ and $b = 3$ mm. The selected values of the collector performance parameters $(\tau\alpha)_n = 0.85$ and $U_L = 8\ \mathrm{W\,m^{-2}\,K^{-1}}$ correspond to a conventional single glazing flat plate collector design. To simplify the comparison, the temperature distribution in the flow direction of the collector was completely ignored, so the Hottel–Willier–Bliss model in terms of the average fluid temperature T_f becomes,

$$\eta = (\tau\alpha)_n F' - U_L F'[(T_f - T_a)/G] \tag{24}$$

In the same plot, the performance line for an ordinary single glazing flat plate collector with a conventional copper sheet absorber was comparatively plotted by a dotted line for identical $(\tau\alpha)_n$ and U_L parameters. In this case, for a 1 mm sheet and 10 mm diameter copper tubes 6 cm apart, the theory [5] predicts that $F' = 0.872$, which leads to $(\tau\alpha)_n F' = 0.741$ and $U_L F' = 6.976\ \mathrm{W\,m^{-2}\,K^{-1}}$. As is comparatively shown, there is an appreciable, almost 14%, performance improvement for the back compared to the top absorbing plate collector, which has a collection efficiency almost identical to that of an ordinary metal absorber.

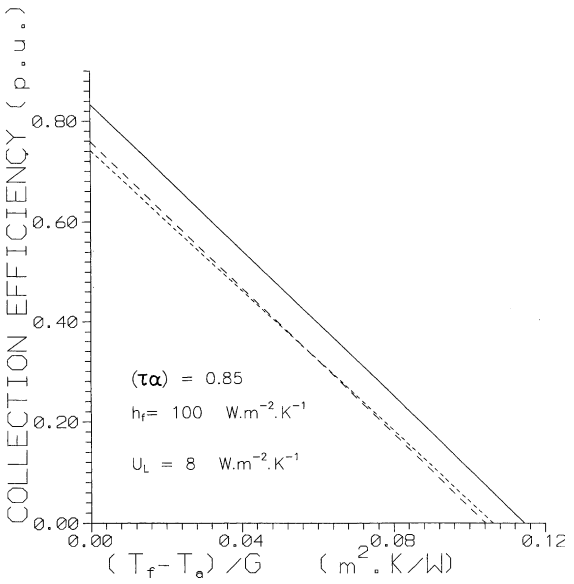

Fig. 8. Comparative presentation of the instantaneous heat collection efficiency of a solar collector with a back absorbing (solid line) and top absorbing (broken line) parallel plate polymer absorber for $b = 3$ mm. In the same plot, the comparative performance of a conventional plate and tube, metal absorber collector design is shown (dotted line) for $(\tau\alpha)_n = 0.85$, $h_f = 100$ and $U_L = 8\ \mathrm{W\,m^{-2}\,K^{-1}}$.

5. Conclusions

Although polymers are potential low cost materials suitable for mass production of low cost modular solar arrays, their general characteristic of low thermal conductivity makes them marginally suitable for the design and manufacturing of polymer solar energy absorbers, unless a suitable design can be employed. Among the various designs, the extruded polymer plate absorber appears to be very suitable for large, all polymer, low cost collector modules. However, owing to the low thermal conductivity of polymer plates, there are certain design limitations for the top absorbing plate absorber, which can be completely eliminated when the top plate of the extruded parallel plate absorber is transparent.

The present investigation was devoted to evaluation of the performance parameters for a collector with a fully wetted, back absorbing, parallel polymer plate absorber design. This improved absorber design allows absorption of the radiation at the back polymer plate and in the flowing water stream, something which eliminates the adverse effects of the low top absorbing plate conductance on collector performance and leads to an improved collector efficiency. According to the derived results, the collector efficiency factor and the collector loss coefficient for the collector with a back absorbing plate absorber is almost 20% higher and about 15% lower than the corresponding parameters for the top absorbing plate absorber. This collector efficiency factor improvement and collector loss coefficient reduction were found to lead to a substantial instantaneous collector heat collection efficiency increase in the order of 14%, uniformly over a wide range of operating conditions.

References

[1] Guinn GR, Hall BR. Solar production of industrial process hot water using shallow solar ponds. Proc Solar Industrial Process Heat Symp., 1977. p. 161–9.
[2] Casamajor AB. The application of shallow solar ponds for industrial process heat: case histories. Proc AS/ISES Silver Jubilee Congress, Atlanta, GA, 1979. p. 1029–32.
[3] Clark AF, Dickinson WC. Shallow solar ponds. In: Dickinson WC, Cheremisinoff PN, editors. Solar energy technology handbook: part A. New York: Marcel Decker; 1980. p. 377–402.
[4] Tsilingiris PT. Design, analysis and performance of low-cost plastic film large solar water heating systems. Solar Energy 1997;60(5):245–56.
[5] Duffie JA, Beckman WA. Solar engineering of thermal processes. New York: Wiley; 1980.
[6] Tsilingiris PT. Heat transfer analysis of low thermal conductivity solar energy absorbers. Appl Thermal Engng 2000;20:1297–314.
[7] Waksman D, Dawson A. The influence of environmental exposure on solar collectors and their materials. Proc AS/ISES Conf 1980;3.1:415–9.
[8] Best D. New plastics head for higher temperatures, Solar Age 1982:51–2.
[9] Baumaister Th, Avallone E, editors. Mark's standard handbook for mechanical engineers. New York: McGraw Hill; 1978.
[10] Materials reference issue, Machine Design, 1979;51(6).
[11] Gartman H, editor. De Laval engineering handbook. New York: McGraw Hill: 1970.
[12] Madsen P, Goss K. Report on nonmetallic solar collectors. Solar Age 1981;6(1):28–32.
[13] Dietz AGH. In: Hamilton RW, editor, Diathermanous materials and properties of surfaces in space heating with solar energy, Cambridge, MA: MIT Press; 1954. p 25–43.
[14] Fundamental materials considerations for solar collectors. Zerlaut GA. In: Dickinson WC, Cheremisinoff PN, editors. Solar energy technology handbook,: part B. New York: Marcel Decker; 1980. p. 403–37.
[15] Du Pont Company, TEDLAR PVF film Technical Bulletin TD-5, 1985.
[16] Incropera F, DeWitt D. Fundamentals of heat and mass transfer, New York: Wiley; 1985.
[17] Kays WM. Convective heat and mass transfer. New York: McGraw-Hill; 1966.
[18] Tsilingiris PT. An accurate upper estimate for the transmission of solar radiation in salt gradient ponds. Solar Energy 1988;40(1):41–8.
[19] Tsilingiris PT. On optical performance and directional characteristics of plastic film liquid layer solar water heaters. Solar Energy 1998;63(5):293–302.